Available online at www.sciencedirect.com
ScienceDirect
Trans. Nonferrous Met. Soc. China 27(2017) 2090−2095
Transactions of Nonferrous Metals Society of China
www.tnmsc.cn

Synthesis and alumina leaching mechanism of calcium sulphoaluminate

Bo WANG[1,2], Wei-qin CHU[1], Yuan-liang HAO[1], Shuo RONG[1], Hui-lan SUN[1,2]

1. School of Materials Science and Engineering, Hebei University of Science and Technology, Shijiazhuang 050018, China;
2. Hebei Key Laboratory of Material Near-net Forming Technology, Hebei University of Science and Technology, Shijiazhuang 050018, China

Received 19 January 2016; accepted 28 September 2016

Abstract: Calcium sulphoaluminate ($3CaO·3Al_2O_3·CaSO_4$, abbreviated as C_4A_3S) was synthesized by sintering at 1375 °C for 2 h with analytically pure carbonate calcium, alumina and dihydrate calcium sulfate. The crystal structure of C_4A_3S was characterized by XRD, SEM and TEM. Alumina leaching properties in Na_2CO_3 solution were studied, and the leaching mechanism was investigated by means of Raman spectrum and XRD. The results show that C_4A_3S has porous morphology. The polycrystallines and single crystals coexist in C_4A_3S and grow along different directions. The alumina leaching rate of C_4A_3S is 98.41%, which is higher than that of $12CaO·7Al_2O_3$ under the optimal condition. The aluminum and sulfur elements exist in the leaching solution in the form of $Al(OH)_4^-$ and SO_4^{2-}, respectively, and the calcium exists as $CaCO_3$ in the leaching residues.

Key words: calcium sulphoaluminate; synthesis; alumina; leaching

1 Introduction

With the continuous improvement of the global industrial production, alumina industry has been rapidly developed [1]. The alumina production of China increased to 5125 million tons in 2014 from 700 million tons in 2004 [2]. The ore grade decreases because of the sharp and increasing demand of bauxite. It's meaningful to study the use of non bauxite resources (such as red mud, fly ash, and iron-bearing bauxite) in the production of alumina [3]. So, the comprehensive utilization of the low grade ore, fly ash and solid waste has become research hotpots [4−7].

At present, for low grade ore, red mud and fly ash whose A/S (Al_2O_3/SiO_2, mass rate) is less than or equal to 3, the lime sintering method has many advantages, such as high alumina leaching rate, low level of secondary reaction, dry sintering process without alkali [8,9]. The main aluminum phase of lime sinter process is $12CaO·7Al_2O_3$ whose alumina leaching property is excellent [10]. However, it also owns a lot of shortcomings, such as large consumption of calcium oxide, large material flow, considerable amount of slag, and small burning temperature range. Based on our previous study, the alumina leaching rate can reach 95% in the process of treating fly ash with lime sintering process, but the main phase of the clinker is C_4A_3S but not $12CaO·7Al_2O_3$, which is consistent with the research of GOODBOY [11]. He found that C_4A_3S clinker has a good alumina leaching property. It substitutes $12CaO·7Al_2O_3$ as the main phase while the C/A (molar rate between CaO and Al_2O_3) decreases from 1.71 to 1.33, and a high alumina leaching property is achieved under the condition of low calcium and aluminum. The source of sulfur of the process is calcium sulfate, which is the desulfurization residue obtained during the burning of pulverized coal. Therefore, it is very important to study the synthesis and the alumina leaching of C_4A_3S. At present, the researches on C_4A_3S are mainly focused on the cement, because C_4A_3S is the main component of the sulfate cement clinker and it has a fast hydration and good sulfur retention characteristics [12−14]. The formation of C_4A_3S is hindered with the increase of the concentration of additives, such as P_2O_5 and Cr_2O_3 [15]. The use of phosphorus gypsum can significantly reduce

Foundation item: Project (E2016208107) supported by the Natural Science Foundation of Hebei Province, China; Projects (QN2015002, BJ2016023) supported by the Science and Technology Foundation of Higher Education Institution of Hebei Province, China
Corresponding author: Bo WANG; Tel: +86-311-81668705; E-mail: wangbo1996@gmail.com
DOI: 10.1016/S1003-6326(17)60234-6

the temperature and time of the formation of C_4A_3S compared with the use of gypsum [16]. LI et al [17] found that the optimal temperature range of formation of C_4A_3S with C_3S and $CaSO_4$ was 1150−1350 °C, and the corresponding optimum holding time was 1−6 h. It was also found that the holding time decreased with the increase of the sintering temperature. The reaction equation is

$$3Ca_3Al_2O_6+CaSO_4 \longrightarrow Ca_4Al_6O_{12}(SO_4)+6CaO \quad (1)$$

The formation mechanism [18] and the thermodynamics [19] and kinetics of C_4A_3S [20] were researched, and the formation reaction of C_4A_3S was determined as

$$CaSO_4+3CaO+3Al_2O_3 \longrightarrow 3CaO\cdot 3Al_2O_3\cdot CaSO_4 \quad (2)$$

Therefore, the researches on the formation and hydration of C_4A_3S are widely reported, but the alumina leaching properties and mechanism are rarely reported. In order to eliminate the influence of other impurities, the pure C_4A_3S was synthesized by adding calcium sulfate as the source of sulfur in this work. The structure of C_4A_3S was characterized, and the alumina leaching behavior and mechanism were studied to provide a theoretical basis for the treatment of low sulfur grade raw materials with lime sintering process.

2 Experimental

2.1 Materials

The synthesis experiment of C_4A_3S was carried out with the analytically-pure reagents of carbonate calcium, alumina and dihydrate calcium sulfate.

The alumina leaching solution was prepared by analytically pure reagents of sodium carbonate and sodium hydroxide solution.

2.2 Experimental apparatus

Experimental apparatus: KSL-1700X-A2 box type high temperature sintering furnace, thermostatic water bath, SFM-1 planetary ball mill, planet type mixer.

Analytical apparatus: D/MAX-2500 X-ray diffraction analyzer of Rigaku made in Japan, S-4800-I scanning electron microscopy (SEM) of HITACHI made in Japan, JEM-2100 transmission electron microscopy (TEM) of JEOL made in Japan and Nicolet 6700 FT-Raman modules of Thermo Fisher made in America.

2.3 Synthesis of C_4A_3S

According to the formula of C_4A_3S, analytically pure carbonate calcium, alumina and dihydrate calcium sulfate were weighed at the rate of 3:3:1. They were mixed in the planetary mixer at the speed of 130 r/min for 2 h. The mixed material was sintered for 2 h at 1375 °C and then was taken out when the temperature below 200 °C. After sintering process, a portion of the sintered clinker was ground to less than 200 meshes (≤74 μm) for the use of XRD analysis and alumina leaching in the SFM-1 planetary ball mill at the speed of 250 r/min for 1 h. The scanning angle of XRD ranged from 10° to 80°, and the scanning speed was 2 (°)/min. Another part of the sintered sample was polished, corroded, sprayed with gold, and scanned by the SEM.

2.4 Alumina leaching of C_4A_3S

The leaching experiments of clinker were carried out in the constant temperature water bath, using flask as leaching container which was connected with the circulating cooling water. The experiments were performed under the following conditions: carbon alkali concentration (N_C) was 80 g/L, caustic concentration (N_K) was 10 g/L, leaching temperature ranged from 60 to 90 °C, leaching time ranged from 5 to 30 min, liquid to solid rate (L/S) was 10, and stirring speed was 400 r/min. The content of Al_2O_3 in the filtrate was analyzed by EDTA titration, and the content of SO_4^{2-} was analyzed by Barium sulfate gravimetric method. The alumina leaching rate was calculated according to

$$\eta_{AO}=\frac{C_{ls}\cdot V_{ls}-C_{cl}\cdot V_{cl}}{m\cdot w} \quad (3)$$

where C_{ls} is the alumina content in leaching solution, g/L; C_{cl} is the alumina content in correction liquor, g/L; V_{ls} is the volume of leaching solution, L; V_{cl} is the volume of correction liquor, L; m is the mass of C_4A_3S, g; w is the alumina mass fraction of C_4A_3S.

3 Results and discussion

3.1 Synthesis of C_4A_3S

A part of the sintered sample was analyzed by XRD. The XRD pattern is shown in Fig. 1. Another part of the sintered sample was scanned by the SEM. The result is shown in Fig. 2.

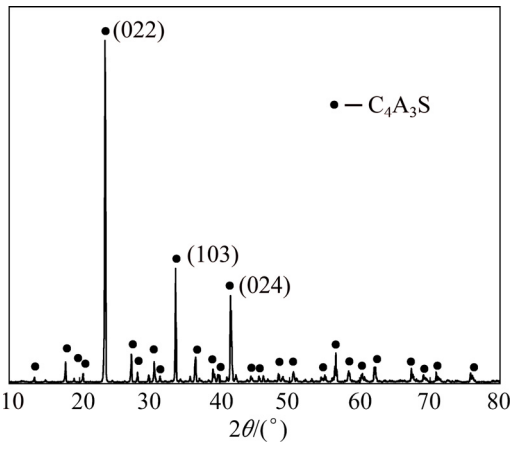

Fig. 1 XRD pattern of sintering clinker at 1375 °C for 2 h

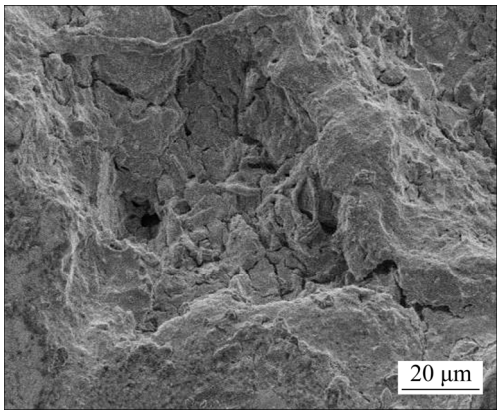

Fig. 2 SEM image of C_4A_3S

The result of X-ray analysis shows that single phase C_4A_3S (PDF card number 85-2210) is obtained under the sintering conditions, and there is no impurity phase. The intensity and half height width of the strongest peak are 15499 and 0.146, so the crystallinity of C_4A_3S is high. The SEM image shows that its micro-morphology is porous, and there are some big gaps, as illustrated in Fig. 2. These pores can increase the contact area of the solid reaction and increase the reaction rate in the process of leaching.

A part of the sample was milled to below 100 nm, and then the ultrasonic dispersion was carried out for TEM analysis. The selected area electron diffraction (SAED) and lattice fringe image of C_4A_3S are shown in Fig. 3.

Because the electron diffraction pattern of Fig. 3(b) is a series of different radii of the concentric rings, there are some polycrystallines in C_4A_3S. But the diffraction pattern (Fig. 3(c)) indicates a single crystal, so the C_4A_3S is a coexisting phase of polycrystallines. Figures 3(c) and (d) show that C_4A_3S mainly has two growth directions, and their interplanar spacings are 0.3635 and 0.2936 nm. And combined with XRD results, the preferred orientations of C_4A_3S are (022) and (103), respectively, which are the strongest and the second strongest peaks of C_4A_3S.

The results of XRD, SEM and TEM analysis show that the microstructure of the C_4A_3S synthesized at 1375 °C for 2 h is porous and it grows in different directions.

3.2 Leaching mechanism of C_4A_3S

3.2.1 Alumina leaching of C_4A_3S

The effect of temperature on the leaching performance of C_4A_3S was studied under the leaching conditions (N_C=80 g/L, N_K=10 g/L, leaching time: 30 min, stirring speed: 400 r/min, and L/S=10). The results are shown in Fig. 4.

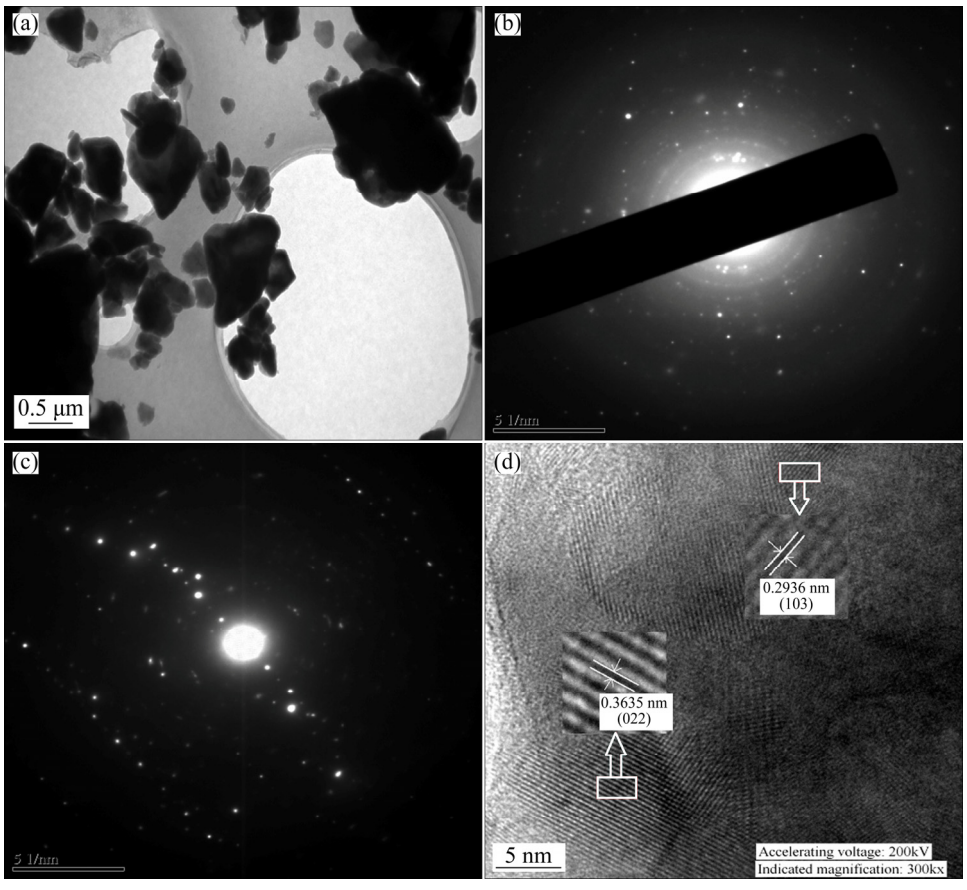

Fig. 3 TEM image of C_4A_3S (a), selected area electron diffraction patterns of C_4A_3S (b) and (c), and HRTEM image of C_4A_3S (d)

As shown in Fig. 4, the leaching rate of C_4A_3S increases obviously with the increase of temperature from 60 to 80 °C. After that, the effect of temperature on leaching rate decreases. And the leaching rate remains up to 98%. Therefore, C_4A_3S can be easily leached out and its optimal leaching temperature is 80 °C.

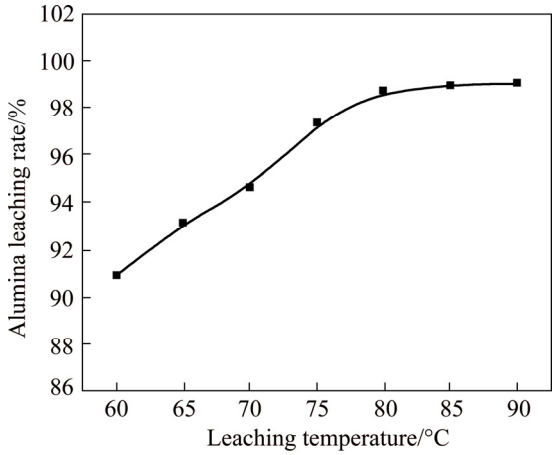

Fig. 4 Effect of leaching temperature on alumina leaching rate of C_4A_3S

The effect of leaching time on the leaching performance of C_4A_3S was investigated under the leaching conditions (N_C=80 g/L, N_K=10 g/L, leaching temperature: 80 °C, stirring speed: 400 r/min, and L/S=10). The results are shown in Fig. 5.

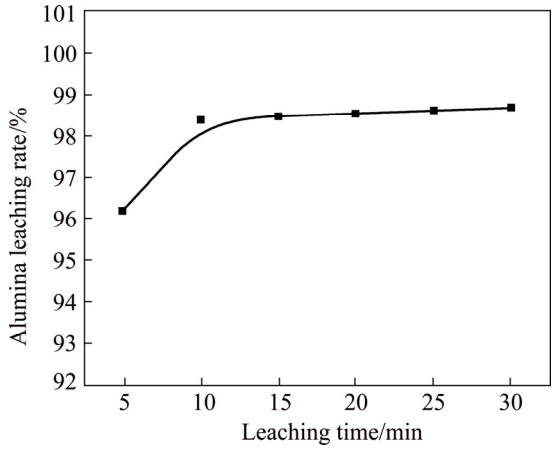

Fig. 5 Effect of leaching time on alumina leaching rate of C_4A_3S

As can be seen in Fig. 5, C_4A_3S can be leached in a short period of time, and the leaching rate is high. After 10 min leaching, the leaching rate changes little. As illustrated in Fig. 2, the micro-morphology of C_4A_3S is porous, which increases the contact area of the liquid and solid, accelerates the reaction rate and makes the reaction more adequate.

Based on the leaching experiments, the optimum leaching conditions (N_C=80 g/L, N_K=10 g/L, leaching temperature: 80 °C, leaching time: 10 min, stirring speed: 400 r/min, and L/S=10) are confirmed. Under those conditions, the alumina leaching rate of C_4A_3S is 98.41%. However, the alumina leaching rate of $12CaO·7Al_2O_3$ is 93.30% under the conditions of N_C=80 g/L, leaching temperature: 80 °C, and leaching time: 30 min [21]. This indicates that the leaching performance of C_4A_3S is better than those of $12CaO·7Al_2O_3$. And also, the leaching time and C/A of C_4A_3S are shorter and lower than that of $12CaO·7Al_2O_3$. Therefore, this process can save the lime consumption and energy during the leaching process.

3.2.2 Leaching mechanism analysis

The alumina leaching experiment of the C_4A_3S was carried out under the optimum leaching conditions of the section 3.2.1. Raman spectrum analyses of the correction liquor and the leaching solution were also carried out. The results are shown in Figs. 6 and 7.

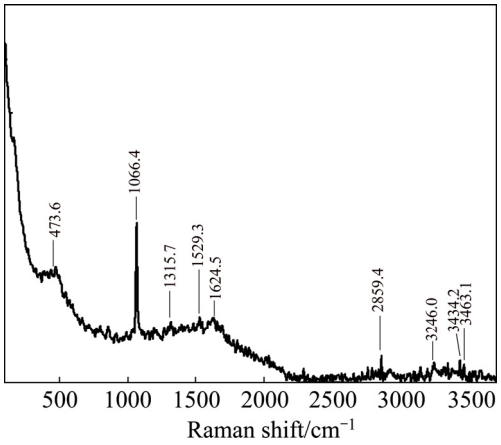

Fig. 6 Raman spectrum of correction liquor before leaching

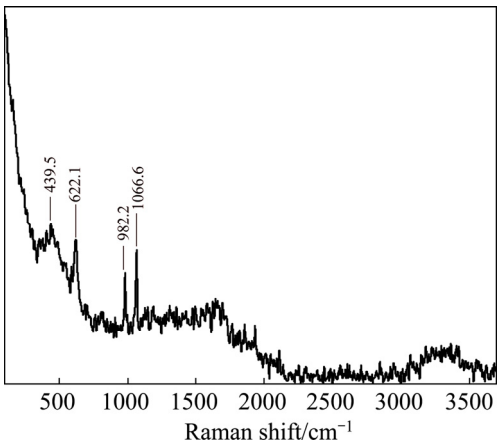

Fig. 7 Raman spectrum of C_4A_3S leaching solution

The concentration of SO_4^{2-} ion in the solution was 0.047 mol/L determined by gravimetric method. It's closed to the theoretical value of 0.048 mol/L. And, the characteristic peak of SO_4^{2-} is found at 982.2 cm^{-1} in Fig. 7 [22]. Therefore, the sulfur element in the clinker

basically exists in the leaching solution in the form of SO_4^{2-} ion. The result shows that the characteristic peak of Al—OH stretching vibration band of $Al(OH)_4^-$ structure is at 622 cm^{-1} in Fig. 7 [23]. Namely, $Al(OH)_4^-$ is generated after leaching. The characteristic peaks of CO_3^{2-} are found at 1315.7 cm^{-1} (Fig. 6) and 1066 cm^{-1} (Fig. 7) [24]. It can be seen from Fig. 7 that there is no sharp peak at 1315.7 cm^{-1}, because a part of Na_2CO_3 solution is consumed in the reaction process. By comparing Figs. 6 and 7, there is still CO_3^{2-} in the leaching solution at 1066 cm^{-1} (Fig. 7), and the peak is still sharp, but the peak intensity decreases. There is O—H for different structures at 3200−3463.1 cm^{-1} [25]. According to the comparison of the Raman spectra (Figs. 6 and 7), the peak shape of O—H before leaching (Fig. 6) converts to the shoulder peak after leaching and the peak width increases (Fig. 7), mainly due to the change of expansion of O—H by the free stretching to O—H bond stretching vibration.

The X-ray diffraction pattern of the leaching residue was carried out, and the result is shown in Fig. 8.

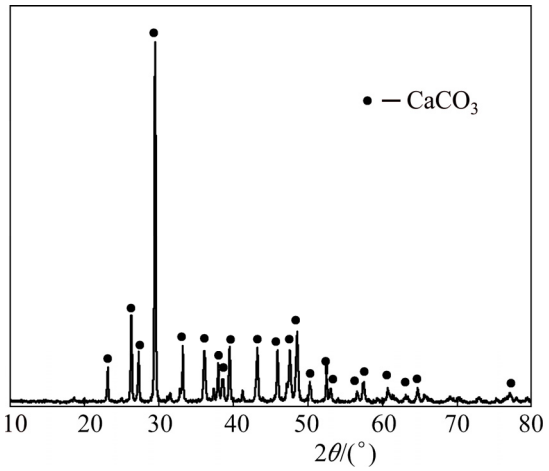

Fig. 8 XRD pattern of leaching residue

Figure 8 shows that C_4A_3S has been completely leached, and there is no aluminiferous compound phase. The main phase of leaching residue is $CaCO_3$. In addition, $CaSO_4$ is also not found in the slag. Therefore, the equation of the alumina leaching of C_4A_3S reaction can be determined as

$$4CaO\cdot3Al_2O_3\cdot SO_3+4Na_2CO_3+2H_2O\longrightarrow 6NaAl(OH)_4+4CaCO_3+Na_2SO_4 \quad (4)$$

This is consistent with the results of the study of GOODBOY [11]. In addition, according to the reaction equation, the molecular proportion (α_k, mole ratio between Na_2O and Al_2O_3 in solution) of the solution is equal to 1 when alkali is not added into the solution before leaching. The solution was unstable and easy to decomposition (Fig. 9), and the leaching rate is reduced by about 20% in the experiment. However, the molecular proportion α_k equals 1.26 when the leaching reagent contains alkali (10 g/L). The solution was stable and not easy to decomposition (Fig. 8).

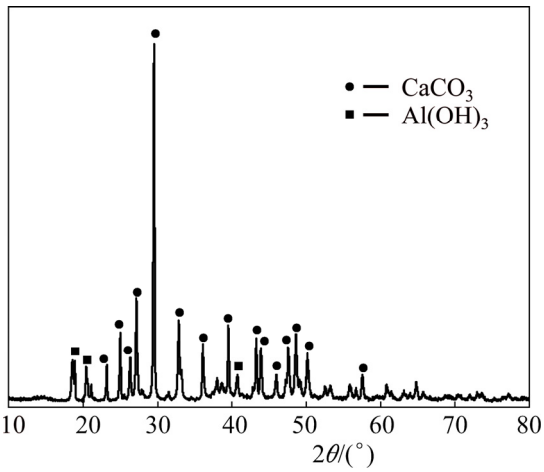

Fig. 9 XRD pattern of leaching residue of C_4A_3S without alkali in correction liquor

From the above analysis, it can be seen that the structure which is Al—OH stretching vibration band of $Al(OH)_4^-$ is generated by the reaction of C_4A_3S and sodium carbonate solution. And $NaAl(OH)_4$ is easy to break down:

$$NaAl(OH)_4\longrightarrow Al(OH)_3+NaOH \quad (5)$$

On the principle of the movement of chemical equilibrium, the decomposition can be restrained by adding sodium hydroxide solution into the correction liquor.

4 Conclusions

1) Pure C_4A_3S is obtained at 1375 °C for 2 h by analytically pure carbonate calcium, alumina and dihydrate calcium sulfate. The crystalline integrity is better, and it has preferred orientations (022) and (103). It has excellent reaction performance in Na_2CO_3 and NaOH solution because its microstructure is porous, which results in the leaching rate increasing and the leaching time shortening obviously.

2) The alumina leaching rate of C_4A_3S can reach 98.70% which is better than that of $12CaO\cdot7Al_2O_3$ of 93.30% under the optimal conditions (N_C=80 g/L, N_K= 10 g/L, leaching temperature: 80 °C, leaching time: 30 min and L/S=10).

3) The aluminum and sulfur elements exist in the leaching solution in the form of $Al(OH)_4^-$ and SO_4^{2-}, and the calcium element exists as $CaCO_3$ in the leaching residues. Adding alkali can inhibit the decomposition of $Al(OH)_4^-$ in leaching solution.

References

[1] YUE Qiang, WANG He-ming, GAO Cheng-kang, DU Tao, LIU Li-ying, LU Zhong-wu. Resources saving and emissions reduction of the aluminum industry in China [J]. Resources, Conservation and Recycling, 2015, 104: 68−75.

[2] YANG Ji-qian. The actuality and the discussion on bauxite and alumina industry in our country [J]. World Nonferrous Metals, 2006(11): 17−19. (in Chinese)

[3] YAO Z T, XIA M S, SARKER P K, CHEN T. A review of the alumina recovery from coal fly ash, with a focus in China [J]. Fuel, 2014, 120: 74−85.

[4] SUN Yu-zhuang, ZHAO Cun-liang, QIN Shen-jun, XIAO Lin, LI Zhong-sheng, LIN Ming-yue. Occurrence of some valuable elements in the unique 'high-aluminium coals' from the Jungar coalfield, China [J]. Ore Geology Reviews, 2016, 72(1): 659−668.

[5] LIU Zhao-bo, LI Hong-xu. Metallurgical process for valuable elements recovery from red mud—A review [J]. Hydrometallurgy, 2015, 155: 29−43.

[6] MOLDOVEANU G A, PAPANGELAKIS V G. Recovery of rare earth elements adsorbed on clay minerals: II. Leaching with ammonium sulfate [J]. Hydrometallurgy, 2013, 131−132: 158−166.

[7] WANG Bo, SUN Hui-lan, GUO Dong, ZHANG Xue-zheng. Effect of Na_2O on alumina leaching property and phase transformation of MgO-containing calcium aluminate slags [J]. Transactions of Nonferrous Metals Society of China, 2011, 21(12): 2752−2757.

[8] LI Yin-tai, BI Shi-wen, DUAN Zhen-ying, YANG Hong-yi, ZHANG Jing-dong. Discussion on the comprehensive process of gibbsite bauxite in Guangxi [J]. Light Metals, 1992(9): 6−14. (in Chinese)

[9] ZHANG Di, YU Hai-yan, PAN Xiao-lin, ZHAI Yu-chun. Effect of alumina existing formation on mineralogical transformation of sintered clinker with low lime dosage [J]. The Chinese Journal of Nonferrous Metals, 2015, 25(12): 3497−3505. (in Chinese)

[10] SUN Hui-lan, YU Hai-yan, WANG Bo, MIAO Yu, TU Gan-feng, BI Shi-wen. Leaching Dynamics of $12CaO·7Al_2O_3$ [J]. The Chinese Journal of Nonferrous Metals, 2008, 18(10): 1920−1925. (in Chinese)

[11] GOODBOY K P. Investigation of a sinter process for extraction of Al_2O_3 from coal wastes [J]. Metallurgical and Materials Transactions B, 1976, 7(4): 716−718.

[12] MA Bing, LI Xue-run, MAO Yu-yi, SHEN Xiao-dong. Synthesis and characterization of high belite sulfoaluminate cement through rich alumina fly ash and desulfurization gypsum [J]. Ceramics-Silikáty, 2013, 57(1): 7−13.

[13] ARJUNAN P, SILSBEE M R, ROY D M. Sulfoaluminate-belite cement from low-calcium fly ash and sulfur-rich and other industrial by-products [J]. Cement and Concrete Research, 1999, 29(8): 1305−1311.

[14] YANG Tian-hua, ZHOU Jun-hu, CHENG Jun, MA Yi, CAO Xin-yu, CEN Ke-fa. Progress in high temperature phase of sulphoaluminate for desulfuration [J]. Journal of Combustion Science and Technology, 2003, 9(1): 35−39. (in Chinese)

[15] BENARCHID M Y, ROGEZ J. The effect of Cr_2O_3 and P_2O_5 additions on the phase transformations during the formation of calcium sulfoaluminate C_4A_3S [J]. Cement and Concrete Research, 2005, 35(11): 2074−2080.

[16] VALETI G, SANTORO L, GAROFANO R. High-temperature synthesis of calcium sulphoaluminate from phosphogypsum [J]. Thermochimica Acta, 1987, 113(87): 269−275.

[17] LI Xue-run, ZHANG Yu, SHEN Xiao-dong, WANG Qian-qian, PAN Zhi-gang. Kinetics of calcium sulfoaluminate formation from tricalcium aluminate, calcium sulfate and calcium oxide [J]. Cement and Concrete Research, 2014, 55: 79−87.

[18] MA Su-hua, SHEN Xiao-dong, HUANG Ye-ping, ZHONG Bai-qian. Preparation and formation mechanism of calcium sulphoaluminate [J]. Journal of the Chinese Ceramic Society, 2008, 36(1): 78−81.

[19] YANG Tian-hua, LI Run-dong, ZHOU Jun-hu, CEN Ke-fa. Formation thermodynamics of high-temperature phase sulphoaluminate [J]. Thermal Power Generation, 2006(6): 6−9, 67. (in Chinese)

[20] YANG Tian-hua, LI Run-dong, ZHOU Jun-hu, CEN Ke-fa. Formation kinetics of high -temperature phase sulphoaluminate [J]. Journal of Chemical Industry and Engineering, 2006, 57(10): 2327−2331. (in Chinese)

[21] YU Hai-yan, WANG Bo, PAN Xiao-lin, BI Shi-wen. Crystal structure and Al_2O_3 leaching properties of $12CaO·7Al_2O_3$ [J]. Chinese Journal of Engineering, 2015, 37(01): 30−34. (in Chinese)

[22] TORRÉNS-MARTÍN D, FERNÁNDEZ-CARRASCO L. Hydration of calcium aluminates and calcium sulfoaluminate studied by Raman spectroscopy [J]. Cement and Concrete Research, 2013, 47(5): 43−50.

[23] WANG Ya-jing, ZHAI Yu-chun, TIAN Yan-wen, HAN Yue-xin, LIU Lian-li, JI Sheng-li. Infrared and Raman spectrum of aluminate and SiO_2-containing sodium aluminate solutions [J]. The Chinese Journal of Nonferrous Metals, 2003, 13(1): 271−275. (in Chinese)

[24] ZHANG Nai, ZHANG Da-jiang, ZHANG Shui-chang, ZHANG Di-jia. Analysis of the anion Raman characteristics and concentration of salt solution at −170 °C [J]. Science in China Series D: Earth Sciences, 2005, 35(12): 1165−1173. (in Chinese)

[25] SUN Qiang. The Raman OH stretching bands of liquid water [J]. Vibrational Spectroscopy, 2009, 51(2): 213−217.

硫铝酸钙的合成及其氧化铝浸出机理

王 波[1,2]，楚维钦[1]，郝圆亮[1]，荣 朔[1]，孙会兰[1,2]

1. 河北科技大学 材料科学与工程学院，石家庄 050018；

2. 河北科技大学 河北省材料近净成形技术重点实验室，石家庄 050018

摘 要：使用分析纯 $CaCO_3$、Al_2O_3 和 $CaSO_4·2H_2O$ 在 1375 °C 保温 2 h 合成纯硫铝酸钙(简写为 C_4A_3S)，通过 XRD、SEM、TEM 对其晶体结构进行表征。在 Na_2CO_3 溶液体系下研究其氧化铝浸出性能，并通过 XRD、Raman 等分析手段对其浸出机理进行分析。结果表明：在该条件下合成的 C_4A_3S 具有疏松孔洞状微观形貌，并存在沿着不同方向生长的多晶与单晶共存结构；在最佳浸出条件下，浸出率高达 98.41%，优于同条件下 $12CaO·7Al_2O_3$ 的浸出率；浸出后 Al 和 S 元素分别以 $Al(OH)_4^-$ 与 SO_4^{2-} 的形式存在于浸出液中，Ca 以 $CaCO_3$ 的形式存在于浸出渣中。

关键词：硫铝酸钙；合成；氧化铝；浸出

(Edited by Bing YANG)